

Providing a model for estimating the compressive strength of square and rectangular columns confined with a variety of fibre-reinforced polymer sheets

Yaser Moodi, Saeed Farahi Shahri and Seyed Roohollah Mousavi

Abstract

One of the most common ways of strengthening the columns is the confinement of the reinforced concrete columns. So far, several experiments have been conducted on concrete columns confined with fibre-reinforced polymer sheets and the results show that the use of fibre-reinforced polymer sheets increases the compressive strength of the concrete columns effectively. Different models in order to determine the compressive strength of the fibre-reinforced-polymer-confined concrete columns are provided in the previous researches. In this study, a wide range of experimental data for square and rectangular columns confined with a variety of fibre-reinforced polymer sheets has been collected. In order to increase the accuracy in the existing models, a modified model for predicting the compressive strength of square and rectangular columns confined with different fibre-reinforced sheets has been proposed by using the collected data. In the current study, the fibre-reinforced polymer strain efficiency factor and the section shape factor are composed and considered as a unique factor. Considering the fibre-reinforced polymer hoop strain concentration at the affected area including the corners area and the surrounding area of them, this factor has been adopted as a fibre-reinforced polymer averaged hoop strain factor for the whole circumference of the section. Based on the published experimental data, a comparison between the analytical results obtained with the present model and the results of the other models, shows considerably better results of the proposed model described in this study. Moreover, application of the proposed model for behaviour prediction of concrete-filled fibre-reinforced polymer tubes is evaluated in this study and the results show that the proposed model is more accurate than the other models.

Keywords

Columns, compressive strength, fibre-reinforced polymer confinement, strengthening

Introduction

Most of the existing reinforced concrete columns are in need of retrofitting and strengthening for various reasons, including errors during the construction phase, poor design plans, adaptation of structures for different functions, the loss of reinforcement due to corrosion, changes in seismic code requirements, occurrence of strong beam-weak column mechanism and the damages due to natural disasters such as earthquake, wind, flood, etc. In addition, the destruction and rebuilding of these columns are costly and often impractical. It should be noted that the strengthening and retrofitting techniques are affordable and reliable.¹ Fibre-reinforced polymer (FRP) is usually used for

the strengthening of the existing reinforced concrete columns.

In 1995, Nanni and Bradford² performed an experimental study on three types of FRP-wrapped normal strength concrete specimens under uniaxial compressive

Civil Engineering Department, University of Sistan and Baluchestan, Zahedan, Iran

Corresponding author:

Seyed Roohollah Mousavi, University of Sistan and Baluchestan, Daneshgah Street, Zahedan 98155-987, Iran.

Email: s.r.mousavi@eng.usb.ac.ir

loading. With detailed analysis of specimens' stress-strain curves, they showed that two mechanical properties of concrete, namely compressive strength and ductility are increased with confinement of concrete columns by FRP jackets. So far, several experimental studies have been done on the various FRP-confined columns. Also, several theoretical models have been proposed to predict the compressive strength of FRP-confined concrete columns.³⁻¹¹ Lam and Teng³ model and Pham and Hadi⁴ model are two well-known existing models for predicting the compressive strength of FRP-confined rectangular and square concrete columns.

In this study, at first the experimental data for FRP-confined rectangular and square concrete columns are extracted from experimental specimens reported in the literature. Then, with these experimental data, a new model based on the Lam and Teng³ model is provided to predict the compressive strength of FRP-confined rectangular and square concrete columns. In this study, FRP strain efficiency factor (k_ε) and section shape factor (k_a) are composed as a unique factor ($(k_\varepsilon)_{new}$), i.e. FRP hoop strain efficiency factor is considered as a function of cross-sectional shape. In Pham and Hadi,⁴ it is assumed that the effective confining stress occurs only at the corners of the cross-sectional area, while in this paper the effects of other regions in the vicinity of the corners are also considered. Thus, a new modified factor is represented for the ratio of stress concentration circumference to the total circumference of cross-sectional shape.

The proposed model is validated by the experimental data. The results show the success of this model in prediction of the compressive strength of FRP-confined rectangular and square concrete columns compared to the other models, so that the total error of the proposed model is averagely decreased about 28.3% for the samples used for modelling phase and about 27% for the samples used for evaluating phase, compared to the other mentioned models. Moreover, the proposed model is used for the concrete-filled FRP tubes.

The results elucidate that the accuracy of the proposed model is better than that of other mentioned models in reproducing the corresponding experimental data, so that employment of the present model for the concrete-filled FRP tubes averagely shows a reduction of 23.2% in the total error compared to those reported by other mentioned models.

Some existing models for the prediction of compressive strength of FRP-confined rectangular and square concrete columns

Lam and Teng³ (ACI 440.2R-08¹²) model

Based on the experimental results, Lam and Teng³ have calculated the compressive strength of FRP-confined

rectangular and square concrete columns (f'_{cc}) as follows

$$f'_{cc} = f'_{co} \left(1 + 3.3k_a \frac{f_{l,a}}{f'_{co}} \right) \quad (1)$$

$$f_{l,a} = \frac{2E_{frp}t_j\varepsilon_{fe}}{D} \quad (2)$$

$$\varepsilon_{fe} = k_\varepsilon\varepsilon_{fu} \quad (3)$$

where f'_{co} is the compressive strength of unconfined concrete; $f_{l,a}$ is the effective lateral confining pressure (equation (2)); ε_{fe} is the FRP actual hoop rupture strain; ε_{fu} is the ultimate tensile strain of FRP jackets; t_j is the total thickness of FRP and E_{frp} is the elastic modulus of FRP materials, respectively. Also, FRP strain efficiency factor is indicated with k_ε and defined by the ratio of FRP actual hoop rupture strain to the ultimate tensile strain of FRP jackets. The factors considered are 0.851, 0.586, 0.624 and 0.788 for the AFRP, CFRP, GFRP and HM-CFRP, respectively. As shown in Figure 1, D is the diameter of an equivalent circular cross-section circumscribing the rectangular section and calculated by the following equation

$$D = \sqrt{b^2 + h^2} \quad (4)$$

In equation (4), h and b are the section depth and width, respectively.

In equation (1), k_a is the section shape factor and depends on two other parameters including the effective confinement area and the aspect ratio (b/h). In a rectangular cross-section, only a part of the concrete is effectively confined by the transverse reinforcement. As shown in Figure 1, in most of the existing models, it is assumed that the effective confinement area of the concrete includes four parabolas, which intersect the corners with an angle of 45°. So, k_a can be defined as follows

$$k_a = \frac{1}{1 - \rho_g} \left(\frac{b}{h} \right)^2 \left[1 - \frac{\left(\frac{b}{h} \right) (h - 2r)^2 + \left(\frac{h}{b} \right) (b - 2r)^2}{3A_g} - \rho_g \right] \quad (5)$$

where r is the corner radius of the section, A_g is the gross area of the column section with rounded corners and ρ_g is the cross-sectional area ratio of the longitudinal steel reinforcement. It should take into account that Lam and Teng³ model was adopted by the ACI 440 Committee (ACI 440.2R-08¹²). The equations presented by Lam and Teng³ have been utilised by ACI 440.2R-08¹² in order to estimate the compressive

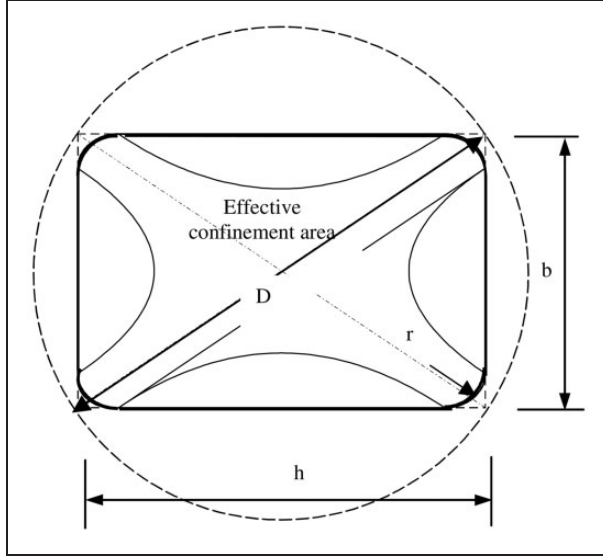


Figure 1. Effective confinement area of the FRP-confined rectangular sections.³

strength of FRP-confined rectangular and square concrete columns with the inclusion of an additional reduction factor $\phi_f = 0.95$.

Pham and Hadi⁴ model

In the paper of Pham and Hadi,⁴ equation (6) is used for the prediction of the compressive strength of FRP-confined rectangular and square concrete columns

$$f'_{cc} = f'_{co} \left(0.68 + 3.91 k_a \frac{f_{l,a}}{f'_{co}} \right) \quad (6)$$

$$f_{l,a} = \frac{E_{frp} t_j \varepsilon_{fe}}{r} \quad (7)$$

In this model, k_ε (FRP strain efficiency factor) is calculated by

$$k_\varepsilon = 0.5 + 0.0642 \ln(A) \quad (8)$$

$$A = \frac{2r}{b R_s} \quad (9)$$

$$R_s = \frac{t_j E_{frp}}{\left(\frac{f'_{co}}{\varepsilon_{co}} \right) r} \quad (10)$$

$$\varepsilon_{co} = (-0.067 f'_{co} 2 + 29.9 f'_{co} + 1053) 10^{-6} \quad (11)$$

In equation (9), R_s is the confinement stiffness ratio obtained from equation (10). Also, in the mentioned study, section shape factor (k_a) is defined as the ratio

of rounded corners total length (in order to avoid the stress concentration) to the whole circumference of the section and it can be represented by the following equation

$$k_a = \frac{\pi r}{b + h - r(4 - \pi)} \quad (12)$$

Some of the other models

To make a more general comparison between proposed model in this study, and the available models in literature for compressive strength prediction of FRP-confined rectangular and square concrete columns, some of the other existing models are summarised in Table 1. The formulations of the Harajli et al.,¹³ Ilki and Kumbasar,¹⁴ Wei and Wu¹⁵ and Toutanji et al.¹⁶ models are presented in Table 1.

Test database

Many investigations have been performed on the FRP-confined concrete. A large test database with 234 FRP-confined square and rectangular specimens is collected from the literature tested by Demers and Neale,¹⁷ Rochette and Labossiere,¹⁸ Parvin and Wang,¹⁹ Pessiki et al.,²⁰ Suter and Pinzelli,²¹ Shehata et al.,²² Ilki and Kumbasar,¹⁴ Masia et al.,²³ Harajli et al.,¹³ Rousakis et al.,²⁴ Al-Salloum,²⁵ Tao et al.,²⁶ Wang and Wu,²⁷ Wu and Wei²⁸ and Wang et al.²⁹ This database covers the FRP-confined square and rectangular specimens with the section width ranging from 79 to 305 mm, the section depth ranging from 100 to 305 mm, the corner radius ranging from 5 to 60 mm and the unconfined concrete strength ranging from 18.3 to 55.2 MPa. Different types of FRP materials such as carbon FRP (CFRP), aramid FRP (AFRP), glass FRP (GFRP) and high modulus carbon FRP (HM-CFRP) are included in the database. All the composite sheets used in the database are oriented in the hoop direction. Monotonic loading is exerted on the collected experimental specimens in this study. Summary of these experimental specimens are listed in Table 2.

The failure mode

Mentioned specimens in the previous section are suddenly failed by the rupture of FRP. In rectangular and square specimens, FRP rupture positions are appeared at the section corners area.^{18,29-31} Thus, the fracture mechanism of the FRP-confined rectangular and square specimens is focused on the FRP hoop stress at the corners. According to Figure 2, the confining

Table 1. Some of the available models for the compressive strength prediction of FRP-confined rectangular and square concrete columns.

Reference	Model	Description
Harajli et al. ¹³	$f'_{cc} = f'_c \left(1 + 1.25 \sqrt{\frac{k_a \rho_f E_{frp} \epsilon_{fe}}{2f'_c}} \right)$	$k_a = 1 - \frac{(b-2r)^2 + (h-2r)^2}{3bh}$ $\rho_f = \frac{4t_j}{D}$, $D = \frac{2bh}{b+h}$
Ilki and Kumbasar ¹⁴	$f'_{cc} = f'_c \left(0.6 + 0.2 \frac{b}{h} \right) \left(1 + 2.29 \left(\frac{f_{l,a}}{f'_c} \right)^{0.87} \right)$	$f_{l,a} = \frac{k_a \rho_f F_{frp}}{2}$, $\rho_f = \frac{2t_j(b+h)}{bh}$ $k_a = 1 - \frac{(b-2r)^2 + (h-2r)^2}{3bh} - \frac{(4-\pi)r^2}{bh}$
Wei and Wu ¹⁵	$f'_{cc} = f'_c \left(1 + 2.2 \left(\frac{2r}{b} \right)^{0.72} \left(\frac{f_{l,a}}{f'_c} \right)^{0.94} \left(\frac{h}{b} \right)^{-1.9} \right)$	$f_{l,a} = \frac{2F_{frp} t_j}{b}$
Toutanji et al. ¹⁶	$f'_{cc} = f'_c + 4 \left(\frac{2r}{D} \right)^{0.1} \left(\frac{h}{b} \right)^{0.13} k_a f_{l,a}$	$f_{l,a} = \frac{2E_{frp} \epsilon_{fe} t_j}{D}$, $D = \frac{2bh}{h+b}$ $k_a = 1 - \frac{(b-2r)^2 + (h-2r)^2}{3bh}$

stress distribution on the section is not uniform. This indicates that the FRP hoop strain in the section corners area has the greatest value and in these regions, FRP reaches its ultimate strain, while in other regions the amount of strain is less than the ultimate strain of FRP.

The proposed model for the compressive strength prediction of the FRP-confined rectangular and square concrete columns

As mentioned in the previous section, the FRP hoop strain at failure experiences the greatest value at the corner regions of specimens. Therefore in this study, it is demonstrated that the FRP strain efficiency factor is a function of section shape for FRP-confined square and rectangular sections. This factor can be calculated by averaging the strains in whole perimeter of the section and it can be utilised for predicting the average FRP hoop stress. For this purpose, it is assumed that strain values are equal to the FRP material ultimate strain at corners and those neighbourhood regions of the section. On the contrary, the other regions have negligible strain values. So, the maximum value is considered for confining stress at the corners and those neighbourhood regions of the section. Although, confining stress is assumed to be zero at the other regions. As shown in Figure 3, there are some segments with αb and βh dimensions where FRP strain reaches to the ultimate strain. As it is described above, the FRP strain

efficiency factor is determined as a function of section shape, using the below equation

$$(k_\epsilon)_{new} = k_a k_\epsilon = \frac{\pi r + \alpha b + \beta h}{b + h - (4 - \pi)r} \quad (13)$$

The best values of α and β coefficients can be obtained by the genetic algorithm optimisation in such a way that the total error (e_{tot}), defined in the following equation, is minimised

$$e_{tot} = \frac{\sum_1^N |Expe_i - Theo_i|}{\sum_1^N |Expe_i|} \quad (14)$$

where $Expe_i$, $Theo_i$ and N are the experimental compressive strength obtained from the experimental database mentioned in the 'Test database' section, compressive strength obtained from the theoretical model and total number of specimens, respectively. However, the proposed model in this study is similar to Lam and Teng³ model, but there are some differences between them. As expressed in equation (13), the proposed model in this study utilises a unique factor instead of the section shape factor and FRP strain efficiency factor in Lam and Teng³ model.

Optimisation is performed on a test database of 234 FRP-confined square and rectangular columns using initial population of 200, total iterations of 20 and α and β values ranging from 0 to 1. The results

Table 2. Summary of FRP-confined square and rectangular concrete specimens for modelling procedure.

Number	Reference	Specimens	Fibre type	Size B (mm) × H (mm)	r (mm)	f_c (MPa)
1	Demers and Neale ¹⁷	5	CFRP, GFRP	152 × 152	5	32.3–42.2
2	Rochette and Labossiere ¹⁸	25	CFRP, AFRP	152 × 152 152 × 203	5, 25, 38	35.8–43.9
3	Parvin and Wang ¹⁹	2	CFRP	108 × 108	8.26	22.6
4	Pessiki et al. ²⁰	2	CFRP	152 × 152	38	26.4
5	Suter and Pinzelli ²¹	16	CFRP, GFRP, AFRP, HM-CFRP	150 × 150	5, 25	33.9–36.6
6	Shehata et al. ²²	8	CFRP	150 × 150 94 × 188	10	23.7–29.5
7	Ilki and Kumbasar ¹⁴	6	CFRP	250 × 250	40	32.8
8	Masia et al. ²³	15	CFRP	100 × 100 125 × 125 150 × 150	25	21.3–25.7
9	Harajli et al. ¹³	18	CFRP	132 × 132 102 × 176 79 × 214	15	18.3
10	Rousakis et al. ²⁴	14	CFRP, GFRP	200 × 200 150 × 150	5, 30	28.7–40
11	Al-Salloum ²⁵	7	CFRP	150 × 150	5, 25, 38, 50	26.7–31.8
12	Tao et al. ²⁶	24	CFRP	150 × 150 150 × 230 150 × 300	20, 35, 50	19.5–49.5
13	Wang and Wu ²⁷	48	CFRP	150 × 150	15, 30, 45, 60	29.3–55.2
14	Wu and Wei ²⁸	30	CFRP	150 × 150 150 × 188 150 × 225 150 × 260 150 × 300	30	35.3
15	Wang et al. ²⁹	14	CFRP	305 × 305 204 × 305	20, 30	25.5

CFRP: carbon fibre-reinforced polymer; GFRP: glass fibre-reinforced polymer; AFRP: aramid fibre-reinforced polymer; HM-CFRP: high modulus carbon fibre-reinforced polymer.

of optimisation give the values of 0.1996 and 0.0107 for α and β , respectively. It should be noted that the total errors expressed in equation (14) are 13.49% for Lam and Teng³ model and 12.61% for Pham and Hadi⁴ model, while the proposed model gives a total error of 10.70%. It means that the average error of the proposed model is decreased by about 18% compared to that of both Lam and Teng³ and Pham and Hadi⁴ models. This decrease in the error indicates that the proposed model can predict the compressive strength of FRP-confined square and rectangular columns more closely to the experimental results.

Considering the non-zero values obtained for α and β and the difference between the $(k_\varepsilon)_{new}$ in the proposed model with the k_a in Pham and Hadi⁴ model, it can be shown that the strain concentration occurs at corners and their neighbourhood regions. Thus, there is a

confining stress concentration at the mentioned regions, so that unlike the Pham and Hadi⁴ model, the effect of these regions is considered in this proposed model. The proposed model for predicting the compressive strength of FRP-confined square and rectangular columns is represented by the following equations, as follows

$$f'_{cc} = f'_{co} \left(1 + 3.3k_\varepsilon \frac{f_{l,a}}{f'_{co}} \right) \quad (15)$$

$$f_{l,a} = \frac{2E_{frp}t_j\varepsilon_{fu}}{D} \quad (16)$$

$$(k_\varepsilon)_{new} = \frac{\pi r + 0.1996b + 0.0107h}{b + h - (4 - \pi)r} \quad (17)$$

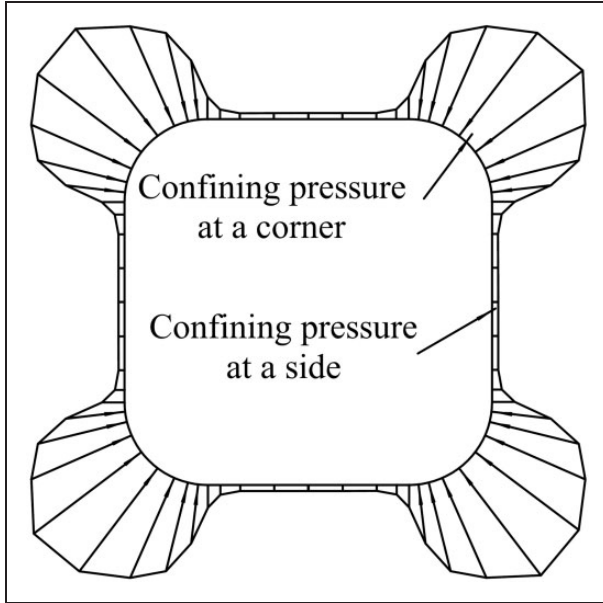


Figure 2. Distribution of confining stress.⁴

where $(k_\epsilon)_{new}$ is the FRP strain efficiency factor, which is considered as a function of the section shape.

Evaluation of the proposed model for compressive strength prediction of FRP-confined rectangular and square concrete columns

In order to evaluate and compare models, a series of experimental data that does not influence the modelling process, is used. These experimental data are collected from Lam and Teng³ and Abbasnia et al.,^{32–35} and details of the specimens are mentioned in Table 3. Also, the error percentage of Lam and Teng³ model, Pham and Hadi⁴ model and the proposed model for each specimen are reported in Table 3. In most cases, the error percentage of the proposed model is less than that of both Lam and Teng³ and Pham and Hadi⁴ models.

For better comparison of models, their performance is evaluated using statistical indicators. These statistical indicators include: (1) mean square error (MSE), (2) average absolute error (AAE) and (3) standard deviation (SD) and all of them can be defined by equations (18) to (20), respectively

$$MSE = \frac{\sum_1^N \left(\frac{Theo_i - Expe_i}{Expe_i} \right)^2}{N} \quad (18)$$

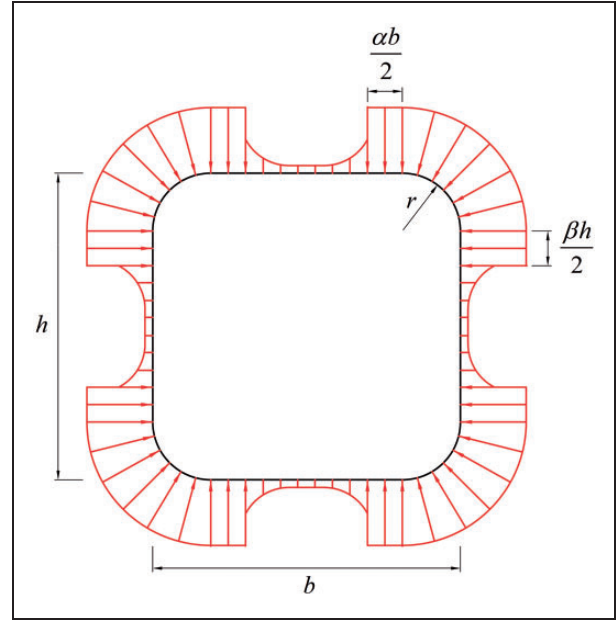


Figure 3. Modified distribution of confining stress.

$$AAE = \frac{\sum_1^N \left| \frac{Theo_i - Expe_i}{Expe_i} \right|}{N} \quad (19)$$

$$SD = \sqrt{\frac{\sum_1^N \left(\frac{Theo_i}{Expe_i} - \frac{Theo_{avg}}{Expe_{avg}} \right)^2}{N - 1}} \quad (20)$$

Calculated statistical indicators required to assess the performance of the proposed model for specimens mentioned in Tables 2 and 3 are summarised in Table 4.

According to the statistical results illustrated in Table 4, the total error of the proposed model decreased by about 26%, 18%, 95%, 11%, 4% and 16% for the specimens used for the modelling step and by about 15%, 20%, 27%, 32%, 40% and 28% for the samples used for the evaluating step, in comparison with the Lam and Teng,³ Pham and Hadi,⁴ Harajli et al.,¹³ Ilki and Kumbasar,¹⁴ Wei and Wu,¹⁵ and Toutanji et al.¹⁶ models, respectively. Figure 4 illustrates the performance of different models for all the specimens mentioned in Tables 2 and 3 with 261 experimental data points. Figure 4 shows the R-squared values of 0.65, 0.70, 0.54, 0.64, 0.73, 0.68 and 0.77 for Lam and Teng,³ Pham and Hadi,⁴ Harajli et al.,¹³ Ilki and Kumbasar,¹⁴ Wei and Wu,¹⁵ Toutanji et al.¹⁶ and the proposed models, respectively. It can be seen that the compressive strength calculated by the proposed model correlated well with the experimental ones. This figure shows the advantage of using the proposed model for the prediction of the

Table 3. Details of the FRP-confined square and rectangular concrete specimens for evaluating procedure.

No.	<i>b</i> (mm)	<i>h</i> (mm)	<i>r</i> (mm)	FRP type ^a	<i>f</i> _{FRP} (MPa)	<i>E</i> _{FRP} (GPa)	<i>t</i> _f (mm)	<i>f</i> _{co} ' (MPa)	<i>f</i> _{cc} ' (MPa)	Error of Lam and Teng model (%)	Error of Pham and Hadi model (%)	Error of proposed model (%)
Lam and Teng ³												
1	150	150	15	C	4519	257	0.17	33.7	35	19.08	13.35	14.99
2	150	150	25	C	4519	257	0.17	33.7	39.4	10.29	7.64	9.50
3	150	150	15	C	4519	257	0.34	33.7	50.4	1.47	6.16	7.14
4	150	150	25	C	4519	257	0.34	33.7	61.9	14.04	4.86	5.03
5	150	150	15	C	4519	257	0.51	24	61.6	22.18	5.28	29.14
6	150	150	25	C	4519	257	0.51	24	66	19.29	0.47	20.69
7	150	150	15	C	4519	257	0.66	24	63.7	13.70	7.69	22.41
8	150	150	25	C	4519	257	0.66	24	80.8	23.43	2.43	24.91
9	150	150	15	C	4519	257	0.825	41.5	82.9	3.23	14.05	11.60
10	150	150	25	C	4519	257	0.825	41.5	95.2	6.68	12.79	8.25
11	150	225	15	C	4519	257	0.66	41.5	49.2	4.91	45.81	16.82
12	150	225	25	C	4519	257	0.66	41.5	51.9	3.51	53.36	23.95
Abbasnia and Ziaadiny ³²												
13	152	152	29	C	4000	240	0.176	30	58.86	33.18	34.21	32.84
14	152	152	29	C	4000	240	0.176	27	61.76	41.17	40.80	40.85
Abbasnia et al. ³³												
15	150	150	13.6	C	3943.5	241	0.352	33	44.395	5.69	11.01	0.61
16	150	150	22.6	C	3943.5	241	0.352	33	48.7129	2.45	10.82	0.14
17	150	150	34.5	C	3943.5	241	0.352	33	49.964	6.38	17.29	10.78
18	150	150	42	C	3943.5	241	0.352	33	55.4919	1.24	10.13	7.68
Abbasnia et al. ³⁴												
19	152	152	29	C	3943.5	241	0.704	50	60	44.67	62.60	45.98
20	90	152	17.5	C	3943.5	241	0.528	30	53.4	23.72	41.49	4.04
21	90	152	17.5	C	3943.5	241	0.528	30	67.5	39.65	11.94	17.69
Abbasnia et al. ³⁵												
22	150	150	42	C	3943.5	241	0.352	30	55.4	6.49	6.22	2.44
23	150	150	42	C	3943.5	241	0.352	30	54.1	4.24	8.77	4.90
24	120	180	33.6	C	3943.5	241	0.352	30	52	25.44	9.47	2.83
25	120	180	33.6	C	3943.5	241	0.352	30	50.4	23.07	12.94	0.25
26	90	180	25.2	C	3943.5	241	0.352	30	49.3	28.94	19.69	2.32
27	90	180	25.2	C	3943.5	241	0.352	30	48.3	27.47	22.17	0.30

^aC = CFRP.

Table 4. Statistical indicators for FRP-confined square and rectangular concrete specimens.

Specimens	Theoretical models	MSE	AAE	SD	<i>e</i> _{tot}
Specimens of Table 2	Lam and Teng ³	3.48	13.83	18.75	13.49
	Pham and Hadi ⁴	3.49	13.46	18.03	12.61
	Harajli et al. ¹³	7.48	22.28	22.05	20.87
	Ilki and Kumbasar ¹⁴	2.73	12.10	16.59	11.92
	Wei and Wu ¹⁵	2.5	11.85	25.61	11.18
	Toutanji et al. ¹⁶	2.93	13.01	16.22	12.45
	Proposed model	2.22	11.34	14.76	10.70

(continued)

Table 4. Continued

Specimens	Theoretical models	MSE	AAE	SD	<i>e</i> _{tot}
Specimens of Table 3	Lam and Teng ³	4.52	16.87	19.31	17.09
	Pham and Hadi ⁴	6.00	18.27	21.90	17.82
	Harajli et al. ¹³	6.04	19.45	23.13	18.86
	Ilki and Kumbasar ¹⁴	9.78	20.38	30.76	19.55
	Wei and Wu ¹⁵	7.01	20.75	26.88	20.68
	Toutanji et al. ¹⁶	8.55	19.64	27.90	18.91
	Proposed model	3.50	14.00	18.82	14.8

MSE: mean square error; AAE: absolute average error; SD: standard deviation.

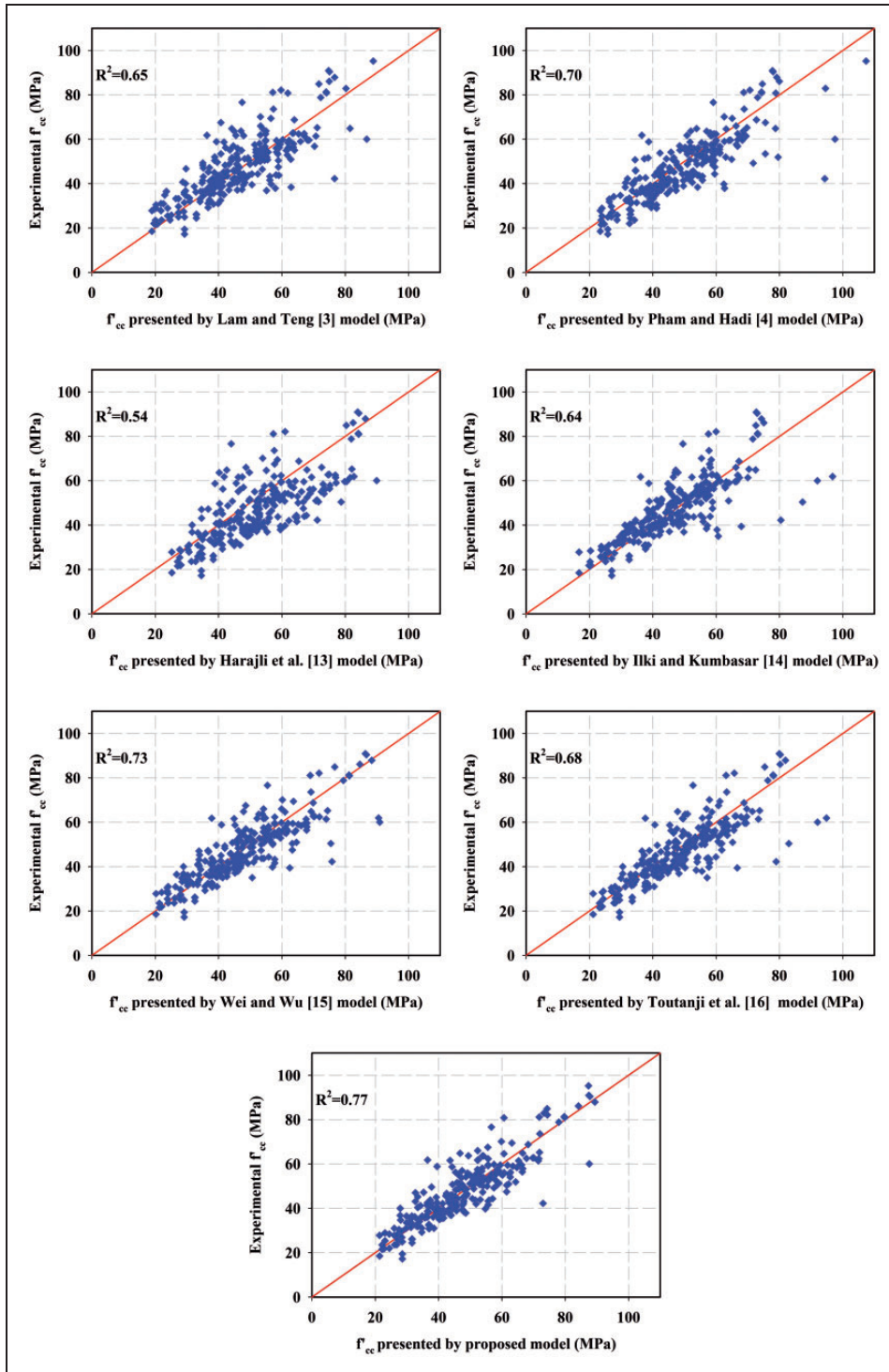


Figure 4. Performance of the selected models.

Table 5. Specimens' summary of the concrete-filled FRP tubes.

Number	References	Specimens	Fibre type	Size		f_c (MPa)
				B (mm) \times H (mm)	r (mm)	
1	Ozbakkaloglu and Xie ³⁶	2	CFRP, GFRP	152.5 \times 152.5	30	21.8–23.5
2	Xie and Ozbakkaloglu ³⁷	3	BFRP	152.5 \times 152.5	30	36.6–38.2
3	Chen and Ozbakkaloglu ³⁸	4	CFRP	150 \times 150	10, 20	38.5
4	Ozbakkaloglu and Oehlers ³⁹	15	CFRP	112.5 \times 225	10, 20, 40	24.0–35.5
				200 \times 200		
5	Ozbakkaloglu ⁴⁰	24	CFRP	150 \times 300	15, 30	76.6–79.6
				150 \times 150		
				126 \times 189		
				112 \times 224		

CFRP: carbon fibre-reinforced polymer; GFRP: glass fibre-reinforced polymer; BFRP: basalt fiber-reinforced polymer.

Table 6. Statistical indicators for the concrete-filled FRP tubes.

Specimen	Theoretical models	MSE	AAE	SD	ϵ_{tot}
Specimens of Table 5	Lam and Teng ³	24.13	28.81	47.29	24.86
	Pham and Hadi ⁴	20.88	41.09	20.31	39.00
	Harajli et al. ¹³	17.73	34.50	25.69	38.62
	Ilki and Kumbasar ¹⁴	9.8	23.72	28.37	25.29
	Wei and Wu ¹⁵	9.38	24.18	28.85	25.01
	Toutanji et al. ¹⁶	11.44	26.31	26.26	28.99
	Proposed model	8.40	22.85	24.78	24.63

compressive strength of FRP-confined square and rectangular concrete columns.

Evaluation of the proposed model for the compressive strength prediction of concrete-filled FRP tubes

In this section, the prescribed relations of section 'The proposed model for the compressive strength prediction of the FRP-confined rectangular and square concrete columns' for the proposed model are verified using the experimental results of the concrete-filled FRP tubes reported by Ozbakkaloglu and Xie,³⁶ Xie and Ozbakkaloglu,³⁷ Chen and Ozbakkaloglu,³⁸ Ozbakkaloglu and Oehlers³⁹ and Ozbakkaloglu.⁴⁰ Table 5 presents the specimens' summary of the concrete-filled FRP tubes. In the mentioned studies, there are some specimens for geopolymer concrete, recycled concrete aggregate and corner strengthening layers, which are not included in Table 5. It should be noted that the strain efficiency factor for basalt fiber-reinforced polymer is not reported in the Lam and Teng³ model. Thus, Lam and Teng³ does not present any prediction for some of the specimens of Table 5.

For better comparison of the three mentioned models, statistical indicators for the specimens of Table 5 are calculated and expressed in Table 6. As shown in Table 6, the prediction of the compressive strength of concrete-filled FRP tubes is improved using the proposed model. So that the total error of the proposed model is approximately decreased by 1%, 58%, 57%, 3%, 2% and 18% compared to the Lam and Teng,³ Pham and Hadi,⁴ Harajli et al.,¹³ Ilki and Kumbasar,¹⁴ Wei and Wu¹⁵ and Toutanji et al.¹⁶ models, respectively.

Conclusions

This study presents a model to predict the compressive strength of FRP-confined square and rectangular columns. In the proposed model, the failure mechanism of the FRP-confined square and rectangular columns is considered such that the actual rupture strain of FRP occurs at corners and those neighbourhood regions of the section. For this purpose, the strain efficiency factor is assumed to be a function of the section shape and it is calculated by averaging the FRP rupture strains in the whole perimeter of the section. The main conclusions of this study can be drawn as follows:

1. The results show that the stress concentration is observed at the corners and those neighbourhood regions of the section, so that unlike the other models, stress concentration in these regions is considered in the proposed model by employment of two coefficients for the section dimensions.
2. The proposed model in this study can predict effectively the compressive strength of FRP-confined square and rectangular columns, so that the total error of the proposed model is averagely decreased by about 28.3% for the samples used for the modelling phase and by about 27% for the samples used

for the evaluating phase, compared to the other mentioned models.

- The prediction of the compressive strength of the concrete-filled FRP tubes using the proposed model is averagely decreased by about 23.2% compared to the other mentioned models.

Declaration of Conflicting Interests

The author(s) declared no potential conflicts of interest with respect to the research, authorship, and/or publication of this article.

Funding

The author(s) received no financial support for the research, authorship, and/or publication of this article.

References

- Ahmad SH, Khaloo AR and Irshaid A. Behavior of concrete spirally confined by fiberglass filaments. *Mag Concrete Res* 1991; 43: 143–148.
- Nanni A and Bradford NM. FRP jacketed concrete uniaxial compression. *Constr Build Mater* 1995; 9: 115–124.
- Lam L and Teng JG. Design-oriented stress-strain model for FRP-confined concrete in rectangular columns. *J Reinf Plast Compos* 2003; 22: 1149–1186.
- Pham TM and Hadi MNS. Stress prediction model for FRP confined rectangular concrete columns with rounded corners. *J Compos Constr ASCE* 2014; 18: 1–10.
- Baji H, Ronagh HR and Li CQ. Probabilistic design models for ultimate strength and strain of FRP-confined concrete. *J Compos Constr ASCE* 2010; 20: 573–582.
- Ziaadiny H and Abbasnia R. Unified cyclic stress-strain model for FRP-confined concrete circular, square and rectangular prisms. *Struct Concr* 2016; 17: 220–234.
- Ozbakkaloglu T, Faggi BAL and Zheng J. Confinement model for concrete in circular and square FRP-concrete-steel double-skin composite columns. *Mater Des* 2016; 96: 458–469.
- Wu YF and Wang LM. Unified strength model for square and circular concrete columns confined by external jacket. *J Struct Eng ASCE* 2009; 135: 253–261.
- Farghal OA and Diab HMA. Prediction of axial compressive strength of reinforced concrete circular short columns confined with carbon fiber reinforced polymer wrapping sheets. *J Reinf Plast Compos* 2013; 32: 1406–1418.
- Ghernouti Y and Rabehi B. FRP-confined short concrete columns under compressive loading: Experimental and modeling investigation. *J Reinf Plast Compos* 2010; 30: 241–255.
- Csuka B and Kollar LP. FRP-confined circular concrete columns subjected to concentric loading. *J Reinf Plast Compos* 2010; 29: 3504–3520.
- American Concrete Institute ACI. Guide for the design and construction of externally bonded FRP systems for strengthening of concrete structures. ACI 440.2R-08, Farmington Hills, MI, USA, 2008.
- Harajli MH, Hantouche E and Soudki K. Stress-strain model for fiber-reinforced polymer jacketed concrete columns. *ACI Struct J* 2006; 103: 672–682.
- Ilki A and Kumbasar N. Compressive behaviour of carbon fibre composite jacketed concrete with circular and non-circular cross-sections. *J Earthq Eng* 2003; 7: 381–406.
- Wei YY and Wu YF. Unified stress-strain model of concrete for FRP-confined columns. *Constr Build Mater* 2012; 26: 381–392.
- Toutanji H, Han M, Gilbert J, et al. Behavior of large-scale rectangular columns confined with FRP composites. *J Compos Constr ASCE* 2010; 14: 62–71.
- Demers M and Neale KW. Strengthening of concrete columns with unidirectional composite sheets. In: Mufti AA, Bakht B and Jaeger LG (eds) *Proceedings of the fourth international conference on short and medium span bridges*. Canadian Society for Civil Engineering, Montreal, Canada, 1994, pp. 895–905.
- Rochette P and Labossiere P. Axial testing of rectangular column models confined with composites. *J Compos Constr ASCE* 2000; 4: 129–136.
- Parvin A and Wang W. Behavior of FRP jacketed concrete columns under eccentric loading. *J Compos Constr ASCE* 2001; 5: 146–152.
- Pessiki S, Harries KA, Kestner JT, et al. Axial behavior of reinforced concrete columns confined with FRP jackets. *J Compos Constr ASCE* 2001; 5: 237–245.
- Suter R and Pinzelli R. Adaptive confinement of concrete columns with FRP sheets. In: *Fifth international conference on fibre reinforced plastics for reinforced concrete structures*, Cambridge, UK, 2001, pp. 793–802.
- Shehata IAEM, Carneiro LAV and Shehata LCD. Strength of short concrete columns confined with CFRP sheet. *Mater Struct* 2002; 35: 50–58.
- Masia MJ, Gale TN and Shrive NG. Size effects in axially loaded square-section concrete prisms strengthened using carbon fiber reinforced polymer wrapping. *Can J Civil Eng* 2004; 31: 1–13.
- Rousakis TC, Karabinis AI and Kiousis PD. FRP-confined concrete members: Axial compression experiments and plasticity modeling. *Eng Struct* 2007; 29: 1343–1353.
- Al-Salloum YA. Influence of edge sharpness on the strength of square concrete columns confined with FRP composite laminates. *Compos Part B: Eng* 2007; 38: 640–650.
- Tao Z, Yu Q and Zhong YZ. Compressive behaviour of CFRP-confined rectangular concrete columns. *Mag Concrete Res* 2008; 6: 735–745.
- Wang LM and Wu YF. Effect of corner radius on the performance of CFRP-confined square concrete columns: Test. *Eng Struct* 2008; 30: 493–505.
- Wu YF and Wei YY. Effect of cross-sectional aspect ratio on the strength of CFRP-confined rectangular concrete columns. *Eng Struct* 2010; 32: 32–45.
- Wang ZY, Wang DY, Smith ST, et al. CFRP confined square RC columns. I: Experimental investigation. *J Compos Constr ASCE* 2012; 16: 150–160.
- Chaallal O, Shahawy M and Hassan M. Performance of axially loaded short rectangular columns strengthened

- with carbon fiber-reinforced polymer wrapping. *J Compos Constr ASCE* 2003; 7: 200–208.
31. Hadi MNS, Pham TM and Lei X. New method of strengthening reinforced concrete square columns by circularizing and wrapping with fiber-reinforced polymer or steel straps. *J Compos Constr ASCE* 2013; 17: 229–238.
 32. Abbasnia R and Ziaadiny H. Behavior of concrete prisms confined with FRP composites under axial cyclic compression. *Eng Struct* 2010; 32: 648–655.
 33. Abbasnia R, Hosseinpour F, Rostamian M, et al. Effect of corner radius on stress–strain behavior of FRP confined prisms under axial cyclic compression. *Eng Struct* 2012; 40: 529–535.
 34. Abbasnia R, Ahmadi R and Ziaadiny H. Effect of confinement level, aspect ratio and concrete strength on the cyclic stress–strain behavior of FRP-confined concrete prisms. *Compos Part B: Eng* 2012; 43: 825–831.
 35. Abbasnia R, Hosseinpour F, Rostamian M, et al. Cyclic and monotonic behavior of FRP confined concrete rectangular prisms with different aspect ratios. *Constr Build Mater* 2013; 40: 118–125.
 36. Ozbakkaloglu T and Xie T. Geopolymer concrete-filled FRP tubes: Behavior of circular and square columns under axial compression. *Compos Part B: Eng* 2016; 96: 215–230.
 37. Xie T and Ozbakkaloglu T. Behavior of recycled aggregate concrete-filled basalt and carbon FRP tubes. *Constr Build Mater* 2016; 105: 132–143.
 38. Chen L and Ozbakkaloglu T. Corner strengthening of square and rectangular concrete-filled FRP tubes. *Eng Struct* 2016; 117: 486–495.
 39. Ozbakkaloglu T and Oehlers DJ. Concrete-filled square and rectangular FRP tubes under axial compression. *J Compos Constr ASCE* 2008; 12: 469–477.
 40. Ozbakkaloglu T. Axial compressive behavior of square and rectangular high-strength concrete-filled FRP tubes. *J Compos Constr ASCE* 2013; 17: 151–161.